ESPI and embedded FBG sensors for composite plate bending measurements

*F.Bosia, G.Zambaz, M.Facchini, J.Botsis, Th.Gmür and P.Giaccari**

Laboratory of Applied Mechanics and Reliability Analysis, Dept. of Mechanical Engineering, and
*Institute of Applied Optics, Dept. of Micro-Engineering
Swiss Federal Institute of Technology,
1015 Lausanne, Switzerland

ABSTRACT
A novel test method combining Electronic Speckle Pattern Interferometry (ESPI) and embedded Fiber Bragg Grating (FBG) sensors is employed to study the out-of-plane and through-the-thickness deformation behaviour of laminated composites. In-house fabricated glass/polypropylene plates are used as specimens. The layers are consolidated in a chosen stacking sequence by compression moulding or by autoclave, thus allowing FBG sensors to be embedded at selected locations between the plies. The specimens are first of all characterized through testing up to fracture in 3-point bending. Measurements are then carried out in the linear elastic range of the material under 3- and 4-point-bending. Full-field surface deformations are derived using in-plane and out-of-plane ESPI, while through-the-thickness axial strains are simultaneously measured using the embedded sensors. Experimental results are compared to those obtained analytically by using classical laminate theory, including the strain variation through the thickness of the plates.

1. INTRODUCTION

1.1 Laminate theories

Composite materials are nowadays of utmost importance in many fields of mechanics, their main advantages being their high stiffness/weight and strength/weight ratios, their tailor-made properties and their processability. However, difficulties remain in their theoretical description, and accurate models for the main structural elements are needed. Laminated composite plates are among these structural elements. They are usually modelled as equivalent single layers with complex constitutive behaviour. The properties of the laminate are derived from the stacking sequence and the properties of the single laminae, the latter modelled as homogeneous orthotropic elastic continua. So-called *equivalent single layer theories* are commonly employed, in order to reduce the 3-D problem to a 2-D one, exploiting the fact that the thickness of a plate is considerably smaller than the planar dimensions. The displacement distribution along the thickness of a deformed plate is then derived from the other two displacement components by adopting suitable hypotheses [1]. For thin plates, the so-called *classical laminated plate theory* (*CLPT*) applies. It is based on the Kirchhoff hypothesis that transverse normals remain straight and perpendicular to the midplane after deformation and are inextensible. In the case of thicker plates, *first* and *higher-order shear deformation theories* must be adopted, whereby shear effects are non-negligeable and the Kirchhoff hypothesis is either relaxed or abandoned altogether.

Very little experimental data exist to date to validate these theories. Moreover, the validity limits of the various approximations have yet to be established. In this study we describe a new non-invasive experimental method using ESPI and FBG sensors to investigate the out-of-plane and through-the-thickness deformation behaviour of composite plates. Preliminary results are presented for thin plates.

1.2 Analytical model

In order to obtain a comparison with experimental results, analytical calculations have been carried out on model laminated plates corresponding to those used in measurements. As a first approximation, the calculations are based on *CLPT*. According to the latter, and having chosen the three coordinates as shown in Fig.1, the displacement field can be expressed as [1]

$$\begin{aligned} u(x,y,z) &= u_0(x,y) - z\frac{\partial w_0}{\partial x} \\ v(x,y,z) &= v_0(x,y) - z\frac{\partial w_0}{\partial y} \\ w(x,y,z) &= w_0(x,y) \end{aligned} \qquad (1.1)$$

where u, v, w are the displacements along x, y, z, respectively, and u_0, v_0, w_0, are the displacements at midplane ($z=0$). In the case of small, linear elastic deformations, the principal strain along the x direction is

$$\varepsilon_{xx} = \frac{\partial u_0}{\partial x} + \frac{1}{2}\left(\frac{\partial w_0}{\partial x}\right)^2 - z\frac{\partial^2 w_0}{\partial x^2} \qquad (1.2)$$

The stresses in the single layers can then be derived from the strains and in turn be related to the global applied moments on the laminate by using plane-stress reduced constitutive relations. In this case the number of independent single-layer material constants is reduced to four, namely E_1, E_2, ν_{12}, G_{12} . We further simplify the problem by adopting a uni-dimensional model and neglecting displacement variations along the y coordinate. This amounts to using beam theory for the calculation of displacements at midplane. The plate curvature along the x direction for symmetrical plates can thus be written as:

$$\frac{\partial^2 w_0}{\partial x^2} = -\frac{M(x)}{E_x I} \qquad (1.3)$$

where *M(x)* is the applied moment in bending, $I=bh^3/12$ is the global moment of inertia, with *b* and *h* respectively the width and thickness of the plate, and *Ex* is the Young's modulus along *x*, which can be derived from the afore-mentioned single-layer constants, the stacking sequence and the plate dimensions. In the case of 3-point bending, the resulting moment on the plate of length *L* is *M(x)=-Px/2* for $x \le L/2$, where *P* is the applied load at the centre of the plate. Given that the first two terms in eq.1.2 are negligeable in our case, the strain distribution can now be estimated to be

$$\varepsilon_{xx} = -\frac{Pxz}{2E_x I} \qquad \left(x \le \frac{L}{2}\right) \qquad (1.4)$$

The strain variation is therefore linear both along *x* and *z.*

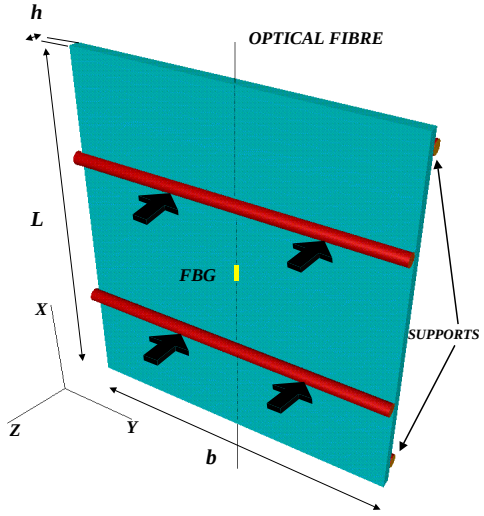

Fig. 1. *Geometry of a specimen subjected to 4-point bending.*

2. EXPERIMENTAL

2.1 Materials and specimen preparation

The specimens chosen for the experimental measurements are in-house fabricated glass-fibre/polypropylene-matrix (galss/PP) laminates from 4/1 woven fabric prepregs, supplied by Vetrotex, France. The weave has 4 fibres in one direction for every fibre in the direction perpendicular to the first. Thus, the single laminae effectively behave as unidirectional layers. The PP matrix is thermoplastic, thus allowing relative simplicity in the fabrication of the specimens, at the cost of some viscoelastic effects appearing in deformation. The prepregs are consolidated together at approximately 10 Bar and 190°C., by means of an appropriate curing cycle, in one of two ways: *a)* compression moulding, *b)* autoclave. For this study, the chosen specimens were 8-ply $(90°/0°)_{2S}$ symmetrical, so-called "cross-ply", laminates. Plate dimensions are 290x250x4.9 mm. The fabrication of laminated plates from prepregs allows the embedding of FBG sensors between plies. The fibres are 125 μm diameter polyimide-coated standard monomode optical fibres. Bragg gratings are written into the fibres by means of a phase mask technique, using a pulsed excimer laser. They are 6 mm in length and the wavelength is centred at approximately 1530 nm. The sensors are placed centrally in the specimens at various locations through the thickness (see sec. 2.5).

2.2 Specimen quality

The porosity of the fabricated specimens is checked through standard ASTM tests and through inspection of optical microscope micrographs of various sections of the material. The void content is found to be at most 2% for autoclave-produced specimens and at most 4% for compression moulded specimens. These are acceptable values and ensure reproducibility in the mechanical properties of the plate specimens. The thickness uniformity of the specimens is then verified. A maximum thickness variation of 1.5% and 3% over the entire plate is obtained for compression-moulded and autoclave-produced specimens, respectively. The exact location of the embedded fibres and their proper alignement is checked by means of X-ray photography on a model specimen in which the optical fibre has been treated with a metallized coating. Micrographs of the section of the specimens are also used to determine the exact depth of the fibre in the laminate after consolidation (Fig.2).

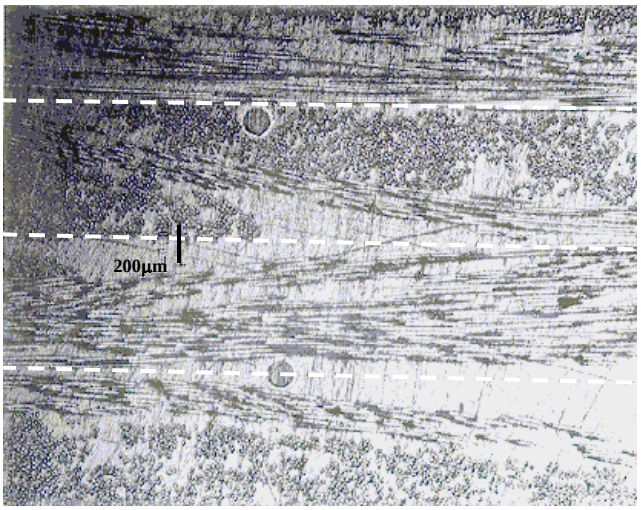

Fig. 2. *Micrograph of a section of a* $(90°/0°)_S$ *laminated plate with two embedded optical fibres. The four layers are distinguishable through morphology, as marked.*

2.3 Specimen characterization

Single-layer material constants have been determined for the glass/PP laminae by means of standard tensile tests and modal identification tests carried out at our laboratory. The following results have been obtained: E_1=24 GPa, E_2=8 GPa, ν_{12}=0.12, G_{12}=1.2 GPa. From these values, the laminate Young's modulus for the chosen stacking sequence is calculated and found equal to 13 GPa.

Three-point-bending tests have been carried out on the specimens by means of an Instron testing system, and load-displacement curves up to fracture have been obtained. The linear elastic range in bending and the resulting plate flexural modulus have been determined for the specimens. Thus, an independent estimation of the Young's modulus E_X can be obtained by using the following relation [2]

$$E_x = \frac{PL^3}{4bh^3\delta}(1+S) \qquad (2.1)$$

where P is the applied load at the centre of the plate and δ is the centre deflection. Here, S is a correction factor due to shear which can be determined by measuring the load-deflection curves for a given specimen using two different support spans. This method yields a value of E_X=12.8±0.3 GPa, in accordance with the previously calculated value.

Finally, the influence of the embedded optical fibres on the mechanical properties of the plates has been assessed. Flexural tests have been carried out on specimens with one or two embedded fibres, and the load-deflection curves compared to those obtained on specimens without embedded fibres. The data show no discernible variation in the three cases, thus leading to the conclusion that the embedded FBG sensors used in this study do not affect the global mechanical response of the specimens.

2.4 ESPI Measurements

The specimens are mounted in a specifically designed loading frame which allows 3- and 4-point bending under various boundary conditions. Simple supports are chosen in this case, with a support span of 250mm. This corresponds to a span/depth ratio of 51, which is usually considered to be typical for the thin plate range. The applied force is measured via a load cell and surface displacements are measured by means of in-plane and out-of plane ESPI [3].

a) Beam specimens. At first, 150x20x4.8mm specimens are considered and horizontal displacements (along the *x* coordinate) are measured on the central part of the lateral free surface (*xz* plane in Fig.1) as the beams are loaded out of plane in 3-point bending. After loading, the CCD camera is displaced laterally in order to remain in line with the original viewing area and to avoid decorrelation. The typical fringe pattern obtained is shown in Fig.3. Clearly to be seen is the central vertical and horizontal neutral lines, where displacements are zero. Processing of the fringe pattern indicates that displacements change sign across the neutral axes, as is to be expected, given that the lower half of the beam is subjected to traction and the upper half to compression. Local delamination effects are to be seen in the lower central half of beam. The results are compared to a calculated fringe pattern, based on the analytical model illustrated above and the resulting displacement field:

$$u(P,x,z) = -\frac{Px^2 z}{4E_x I} + K \qquad (x \le L/2) \qquad (2.2)$$

where K is an integration constant that can be determined in this case by setting *u=0 for x=L/2.*

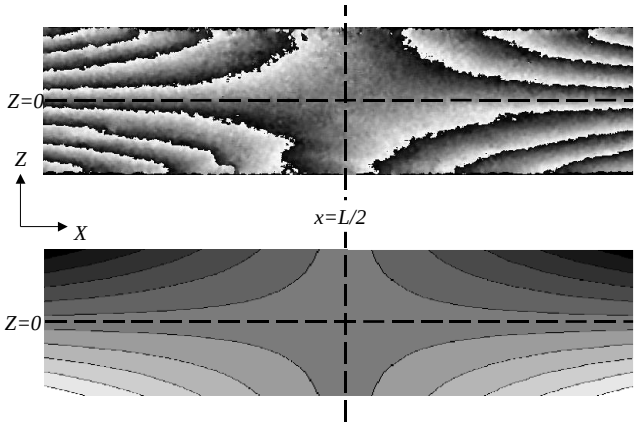

Fig. 3. *Comparison between measured and calculated horizontal in-plane displacement fringes on the lateral surface of the beam.*

The coincidence of the fringe patterns suggests that the adopted analytical approximations are appropriate in this case. Therefore, the thin-plate approximation holds. The experimental displacement distribution *u(z)* has been derived for various fixed *P* and *x* values, and compared to the analytical predictions. Results show that this distribution is indeed linear and that the slope is on average 11.6% greater than that of the analytically predicted distributions. This difference is attributed to the fact that shear effects have been neglected in the theory.

b) Plate specimens. Full field in-plane displacements have also been measured using ESPI on the front surface (*xy* plane in Fig.1) of the plate during 3-point loading, in order to derive the ε_{xx} strain component in the outer surface at the location of the sensor. This strain value is then compared to those measured through the thickness of the composite via FBG (sec. 2.5, Fig. 5). Also, the *u(x)* displacement at the centre of the plate (*y=b/2)* is compared to the predicted quadratic distribution in eq. 2.2 . Here too calculated and measured results differ by an average 10-15%.

Out-of plane ESPI has also been performed on the specimens loaded in 3- and 4- point bending to determine their global deformation and their curvature along *x* at midplane (*y*=*b*/2). A typical deformation profile for 4-point bending is shown in Fig.4. Some asymmetry can be noticed in the profile, attributed to a slight rotation effect due to the loading members. The mean experimental curvature value differs from the analytically predicted one by 12.5%.

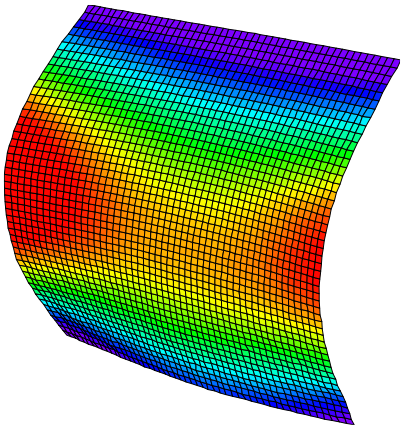

Fig. 4. *Out-of-plane deformation field on a plate specimen.*

2.5 FBG sensor measurements

Embedded FBG sensors provide a reliable tool to measure absolute internal strains in composite materials. The axial strain ε_x in the fibre, which corresponds to the ε_{xx} strain in the host material at the location of the sensor, is related to the Bragg wavelength shift $\Delta\lambda_B$ through the well-known relation

$$\varepsilon_x = \frac{1}{(1-p_e)}\frac{\Delta\lambda_B}{\lambda_B} \qquad (2.3)$$

where λ_B is the Bragg wavelength and (1-p_e) the sensitivity of the fibre [4]. In our case p_e = 0.215±0.010. Measurements were carried out by embedding the sensors as shown in Fig. 1 at different thicknesses in three identical plate specimens. The sensors were placed between layers 1 and 2 in the first specimen, between layers 2 and 3 in the second, and between layers 3 and 4 in the third. Thus, axial strains can be extrapolated through the whole thickness of the laminate, given that it is a symmetric layup and that strains are zero at midplane. The specimens are loaded in 3-point bending and simultaneous FBG and in-plane ESPI (see section 2.4) measurements are carried out. The measured strains show the expected linear dependence with respect to the applied load. Loading and unloading has highlighted the viscoelastic behaviour of the material, and the need for tests to be carried out at an appropriate loading rate. Also, differences between the tensile and compressive behaviour of the material have been found. This is to be expected, as local buckling effects probably play a role in compression. To avoid these effects, and also due to the poorer signal quality in compression, the results considered here refer to the laminate half which is subjected to traction. Figure 5 shows the typical ε_{xx} strain distribution through the thickness of the laminate at a given load, obtained by representing the results from the three specimens on a single graph. Error bars on the FBG measurements essentially derive from the unceirtainty on the exact vertical position of the fibre in the composite. The distribution is fairly linear, but there is some discrepancy with calculated results. The 13.5% difference in the two slopes might indicate a departure from the hypotheses of *CLPT*, but it is hard to tell if this is the case or if the difference is due to the simplified nature of the analytical model.

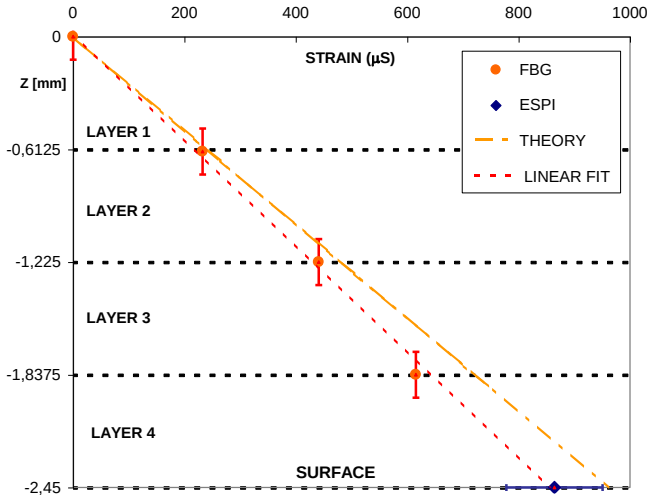

Fig. 5. ε_{xx} *as a function of altitude from midplane for P=200N.*

3. CONCLUSIONS

A novel experimental method using FBG sensors and ESPI has been outlined to determine out-of-plane deformations and through-the-thickness strains in composite laminated plates. Measurements have been carried out on cross-ply specimens with a span/depth ratio of 51. Results show relatively good agreement with calculations based on classical laminate theory, with a deviation of at most 10-15%. Thus, the validity of the method has been proved. Measurements will be carried out in future on thicker plates and results will be compared to numerical simulations in order to reliably assess the validity of the various equivalent-single-layer theories.

ACKNOWLEDGEMENTS

This research is supported by the Swiss National Science Foundation (FNS), grant n. 21-52486.97.

REFERENCES

[1] ***Reddy, J.N.***, *Mechanics of laminated composite plates : Theory and Analysis,* CRC Press, 1997.

[2] ***Fisher, S., Roman, I., Arel, H., Marom, G., and Wagner, H.D.***, *Simultaneous determination of shear and Young's moduli in composites,* Journal of Testing and Evaluation, Vol. 9, No. 5, pp.303-307, 1981.

[3] ***Jones, R., Wykes, C.***, *Holographic and speckle interferometry,* 2nd ed. Cambridge University Press,1983.

[4] ***Measures, R.***, ***"****Smart composite structures with embedded sensors****",*** Composites Engineering, Vol. 2, n. 5-7, pp.597-618, 1992.